UAV-Aided Wireless Communication Design With Propulsion Energy Constraint

Subin Eom, Hoon Lee, Junhee Park and Inkyu Lee, *Fellow*, *IEEE*
School of Electrical Eng., Korea University, Seoul, Korea
Email: {esb777, ihun1, pjh0585, inkyu}@korea.ac.kr

***Abstract*—This paper studies unmanned aerial vehicle (UAV) aided wireless communication systems where a UAV serves uplink communications of multiple ground nodes by flying the area of the interest. In this system, the propulsion energy consumption at the UAV is taken into account so that the UAV's velocity and acceleration should not exceed a certain threshold. We aim to maximize the minimum average rate of the UAV by jointly optimizing the UAV trajectory and the ground nodes' uplink transmit power. However, this problem is shown to be non-convex in general, and thus existing convex optimization techniques and algorithms cannot be directly applied. By employing the successive convex approximation (SCA) techniques, we present an efficient algorithm which is guaranteed to converge to at least a local optimal point for the non-convex problem. To this end, proper convex approximations are derived for the non-convex constraints. Numerical results demonstrate the proposed algorithm performs better than baseline scheme.**

I. Introduction

Recently, unmanned aerial vehicles (UAVs) have been receiving great attention as mobile communication nodes in wireless networks [1]. Compared to conventional terrestrial communications where users are served by ground base stations (BSs) [2], UAV-aided systems are cost effective and can be dispatched to the field with various purposes. In addition, with adjustable mobility, we can optimize deployment and trajectories of moving UAVs in order to maximize the system capacity. Furthermore, located at moderate altitude, UAVs are likely to have line-of-sight (LoS) communication links for air-to-ground channel.

From these advantages, UAVs have been employed to various wireless communication systems. The authors in [3]–[6] considered UAVs as a mobile relay which help ground nodes' communication. In this UAV-aided mobile relaying system, compared to conventional static relay schemes [7], [8], the relay moves closer to source and destination nodes in order to obtain good channel condition, and thus the system throughput can be significantly improved.

In addition, UAVs can help the existing terrestrial communication infrastructure and users [9]–[12]. For the disaster situation, the authors in [9] utilized the UAVs to recover malfunctioned ground infrastructure. In [10], the UAV was adopted to serve the cell-edge mobile users and offload the traffic from the ground BS. The UAV also employed for flying computing cloudlets [11] and a mobile energy transmitter in wireless power transfer systems [12].

Moreover, UAVs could play the role of mobile BS in wireless networks [13]–[16]. The authors in [13] and [14] studied the coverage issue of the mobile BS systems and designed the placement of the UAVs. In [15], theoretical model of the propulsion energy consumption of fixed-wing UAVs was derived. Under this model, energy efficiency of the UAV is maximized for a single ground node system. When there are multiple ground nodes, [16] maximized the minimum throughput performance by jointly optimizing the UAV trajectory, the transmit power, and the time allocations. However, this work did not consider the propulsion energy consumption of the UAV and thus, it may not feasible for fixed-wing UAVs.

This paper studies a UAV-aided wireless communication design, where a UAV collects the data of multiple ground nodes within a finite time period under average propulsion power consumption constraint. We aim to maximize the minimum average rate by jointly optimizing the UAV trajectory, the velocity, and the acceleration as well as the ground nodes' uplink transmit power. Compared to the single ground node scenario in [15], the problem for the general multi-node case in this paper becomes more complicated. Also, since we consider the propulsion energy consumption, unlike the work in [16], additional non-convex constraints should be investigated. As a result, the existing algorithms presented in [15] and [16] cannot be directly applied to our scenario.

To tackle this issue, we first introduce auxiliary variables and transform the non-convex problem into a more tractable formulation. However, the equivalent problem is still non-convex due to the non-convex UAV movement constraints. To this end, we employ the successive convex approximation (SCA) technique which iteratively solves approximated convex problem of the original non-convex one. Novel convex approximations for the non-convex constraints are proposed in order to apply the SCA to our optimization problem. Finally, we present an efficient algorithm for the minimum rate maximization problem which yields at least a locally optimal solution. From simulation result, it is confirmed that the proposed algorithm provides a significant performance gain over baseline scheme.

The rest of this paper is organized as follows. Section II

This work was supported by the National Research Foundation of Korea (NRF) funded by the Korea Government (MSIP) under Grant 2017R1A2B3012316.

978-1-5386-3180-5/18/$31.00 ©2018 IEEE

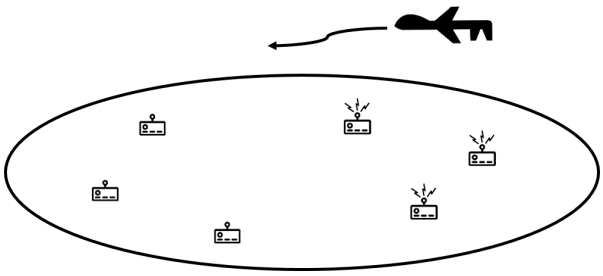

Fig. 1. A UAV-enabled wireless network

introduces the system model and the problem formulation. In Section III, the minimum average rate maximization algorithm is proposed. Section IV presents the numerical results and finally, we conclude the paper in Section V.

Notations: Throughout this paper, the bold lower-case and normal letters denote vectors and scalars, respectively. The space of M-dimensional real-valued vectors are represented by $\mathbb{R}^{M\times 1}$. For a vector $\mathbf{a}$, $\|\mathbf{a}\|$ and $\mathbf{a}^T$ indicate norm and transpose, respectively. The gradient of a function f is defined as ∇f. For a time-dependent function $\mathbf{x}(t)$, $\dot{\mathbf{x}}(t)$ and $\ddot{\mathbf{x}}(t)$ stand for the first-order and second-order derivatives with respect to time t, respectively.

II. System Model And Problem Formulation

A. System Model

As shown in Fig. 1, we consider a UAV-aided wireless communication system where a UAV serves uplink data transmission of K ground nodes as a mobile BS. In this scenario, the UAV horizontally flies at a constant altitude H with a time period T. The ground nodes are assumed to be deployed at fixed location, which is perfectly known at the UAV in advance.

To represent the location of the UAV and the ground nodes, we consider a three-dimensional Cartesian coordinate system. The horizontal coordinate of each ground node k ($k = 1, ..., K$) is denoted by $\mathbf{w}_k = [x_k \ y_k]^T$. Also, we define the time-varying horizontal coordinate of the UAV at time instant t as $\mathbf{q}(t) = [q_x(t) \ q_y(t)]^T$, for $0 \le t \le T$. Then, the instantaneous velocity $\mathbf{v}(t)$ and acceleration $\mathbf{a}(t)$ of the UAV are expressed by $\mathbf{v}(t) \triangleq \dot{\mathbf{q}}(t)$ and $\mathbf{a}(t) \triangleq \ddot{\mathbf{q}}(t)$, respectively. Since we consider periodical operations at the UAV, it follows

$$\mathbf{q}(0) = \mathbf{q}(T), \mathbf{v}(0) = \mathbf{v}(T), \mathbf{a}(0) = \mathbf{a}(T), \tag{1}$$

where (1) implies that the UAV needs to go back to its starting location $\mathbf{q}(0)$ with the same velocity and acceleration after one period T. In addition, the velocity and acceleration of the practical UAV are subject to

$$V_{\min} \le \|\mathbf{v}(t)\| \le V_{\max}, 0 \le t \le T, \tag{2}$$

$$\|\mathbf{a}(t)\| \le a_{\max}, 0 \le t \le T, \tag{3}$$

where $V_{\min}$ and $V_{\max}$ stand for the minimum and the maximum UAV speed constraints in m/sec and $a_{\max}$ indicates the maximum UAV acceleration in m/sec^2. The minimum speed constraint $V_{\min}$ is significantly important for practical fixed-wing UAV designs which need to move forward to remain aloft [15].

The continuous-time expressions in (1)-(3) make analysis and derivations on the UAV system intractable. For ease of analysis, we discretize the time duration T into N time slots with the same time interval $\delta_t = \frac{T}{N}$ [3]. When the discretized time interval δ_t is chosen as a small number, based on the first- and the second-order Taylor approximations, the velocity and the acceleration can be denoted as [15],

$$\mathbf{v}(t+\delta_t) \approx \mathbf{v}(t) + \mathbf{a}(t)\delta_t, 0 \le t \le T, \tag{4}$$

$$\mathbf{q}(t+\delta_t) \approx \mathbf{q}(t) + \mathbf{v}(t)\delta_t + \tfrac{1}{2}\mathbf{a}(t)\delta_t^2, 0 \le t \le T. \tag{5}$$

As a result, the trajectory of the UAV can be successfully approximated by N vector sequences as $\mathbf{q}[n] \triangleq \mathbf{q}(n\delta_t)$, $\mathbf{v}[n] \triangleq \mathbf{v}(n\delta_t)$, and $\mathbf{a}[n] \triangleq \mathbf{a}(n\delta_t)$ for $n = 0, 1, ..., N$. Thus, (4) and (5) can be rewritten by

$$\mathbf{v}[n] = \mathbf{v}[n-1] + \mathbf{a}[n-1]\delta_t, \tag{6}$$

$$\mathbf{q}[n] = \mathbf{q}[n-1] + \mathbf{v}[n-1]\delta_t + \tfrac{1}{2}\mathbf{a}[n-1]\delta_t^2, \tag{7}$$

for $n = 1, ..., N$. Also, the constraints in (1)-(3) become

$$\mathbf{q}[0] = \mathbf{q}[N], \mathbf{v}[0] = \mathbf{v}[N], \mathbf{a}[0] = \mathbf{a}[N], \tag{8}$$

$$V_{\min} \le \|\mathbf{v}[n]\| \le V_{\max}, \text{ for } n = 0, 1, ..., N, \tag{9}$$

$$\|\mathbf{a}[n]\| \le a_{\max}, \text{ for } n = 0, 1, ..., N. \tag{10}$$

For the power consumption at the UAV, we consider the propulsion power consumption which is used for maintaining the UAV aloft and supporting its mobility. A theoretical model for the propulsion power consumption was derived in [15]. For tractable analysis, we use the upper bound of this model, which can be expressed as

$$P_{\text{prop}}[n] = c_1\|\mathbf{v}[n]\|^3 + \frac{c_2}{\|\mathbf{v}[n]\|}\left(1 + \frac{\|\mathbf{a}[n]\|^2}{g^2}\right), \forall n, \tag{11}$$

where c_1 and c_2 are two parameters related to the aircraft design and g = 9.8 m/s^2 is the gravitational acceleration. Note that the power consumption related to the communication processes such as analog-to-digital converter and channel decoding are ignored since they are practically much smaller than the propulsion power.

Now, let us explain the channel model between the UAV and the ground nodes. It is assumed that the communication links from the ground nodes to the UAV are dominated by the LoS links. Moreover, the Doppler effect originated from the UAV mobility is assumed to be well compensated. Then, the effective channel gain $h_k[n]$ from node k to the UAV at time slot n follows the free-space path loss model as [3]

$$h_k[n] = \gamma_0 d_k^{-2}[n] = \frac{\gamma_0}{\|\mathbf{q}[n] - \mathbf{w}_k\|^2 + H^2}, \tag{12}$$

where $\gamma_0 \triangleq \beta_0/\sigma^2$ represents the reference signal-to-noise ratio (SNR) at 1 m with β_0 and σ^2 being the channel power at 1 m and the white Gaussian noise power at the UAV,

respectively. Here, the distance $d_k[n]$ between the UAV and node k at time slot n is written by

$$d_k[n] = \sqrt{\|\mathbf{q}[n] - \mathbf{w}_k\|^2 + H^2}. \tag{13}$$

At time slot n, each ground node k transmits its data signal to the UAV with power $0 \le p_k[n] \le P_{\text{peak}}$, where P_{peak} is the peak transmission power constant at the nodes. Accordingly, the instantaneous achievable rate $R_k[n]$ of node k at time slot n can be expressed as

$$R_k[n] = \log_2\left(1 + \frac{p_k[n]h_k[n]}{1 + \sum_{j=1, j\neq k}^{K} p_j[n]h_j[n]}\right), \tag{14}$$

where the term $\sum_{j=1,j\neq k}^{K} p_j[n]h_j[n]$ represents the interference from all other nodes at time slot n. Therefore, the achievable average rate R_k of node k over N time slots is given by

$$\begin{aligned} R_k &= \tfrac{1}{N}\sum_{n=1}^{N} R_k[n] \\ &= \tfrac{1}{N}\sum_{n=1}^{N} \log_2\left(1 + \tfrac{p_k[n]h_k[n]}{1+\sum_{j=1,j\neq k}^{K} p_j[n]h_j[n]}\right). \end{aligned} \tag{15}$$

B. Problem Formulation

In this paper, we jointly optimize the UAV movement variables $\mathbf{q}[n]$, $\mathbf{v}[n]$, and $\mathbf{a}[n]$ and the ground nodes' uplink transmit power $p_k[n]$ so that the minimum average rate among multiple ground nodes is maximized. The minimum rate maximization problem can be formulated as

$$(P1): \max_{\substack{\{\mathbf{q}[n],\mathbf{v}[n],\mathbf{a}[n]\} \\ \{p_k[n],\tau\}}} \quad \tau \tag{16a}$$

$$s.t. \quad R_k \ge \tau, \forall k, \tag{16b}$$

$$0 \le p_k[n] \le P_{\text{peak}}, \forall k, n, \tag{16c}$$

$$\frac{1}{N}\sum_{n=1}^{N} P_{\text{prop}}[n] \le P_{\text{lim}}, \tag{16d}$$

$$(6) - (10),$$

where P_{lim} in (16d) indicates the propulsion power constraint at the UAV.

In general, (P1) is non-convex problem due to the UAV movement constraints (9), the achievable average rate constraint (16b), and the average propulsion power constraint (16d). Thus, it is not easy to obtain the globally optimal solution. Compared to [16], we additionally consider the propulsion power constraint (16d) in the minimum rate maximization problem (P1), so the problem becomes more complicated.

C. Successive Convex Approximation

In this subsection, we briefly review the SCA technique. Suppose a general non-convex problem with constraints $f_i(\mathbf{x}) \ge 0$ for $i = 1, ..., m$. It is assumed that a feasible region $F = \{\mathbf{x}|f_i(\mathbf{x}) \ge 0, i = 1, ..., m\}$ is a compact set and $f_i(\mathbf{x})$ is differentiable.

Then, At the l-th iteration of the SCA algorithm, the non-convex set F is approximated to proper convex set $\widetilde{F} = \{\mathbf{x}|g_i(\mathbf{x}|\mathbf{x}_l) \ge 0, i = 1, ..., m\}$, where $g_i(\mathbf{x}|\mathbf{x}_l)$ is a surrogate function of $f_i(\mathbf{x})$ with solution $\mathbf{x}_l$ obtained at the l-th iteration. The surrogate function $g_i(\mathbf{x}|\mathbf{x}_l)$ is chosen to satisfy the following three conditions

$$g_i(\mathbf{x}_l|\mathbf{x}_l) = f_i(\mathbf{x}_l), \tag{17}$$

$$\nabla g_i(\mathbf{x}_l|\mathbf{x}_l) = \nabla f_i(\mathbf{x}_l), \tag{18}$$

$$g_i(\mathbf{x}|\mathbf{x}_l) \le f_i(\mathbf{x}). \tag{19}$$

It is well known that the limit of any convergent sequence of $\{\mathbf{x}_l\}$ becomes the KKT point, which implies that we can obtain at least local optimal solution for the original non-convex problem [17], [18].

III. Proposed Algorithm

In this section, we propose an iterative algorithm for solving the problem by applying the SCA method. To tackle the non-convex problem (P1), we first introduce the change of variables as

$$G_k[n] \triangleq p_k[n]h_k[n] = \frac{p_k[n]\gamma_0}{\|\mathbf{q}[n] - \mathbf{w}_k\|^2 + H^2}, \forall k, n, \tag{20}$$

where $G_k[n]$ is a new optimization variable. Also, defining $G_{k,\max}[n]$ as

$$G_{k,\max}[n] \triangleq P_{\text{peak}}h_k[n] = \frac{P_{\text{peak}}\gamma_0}{\|\mathbf{q}[n] - \mathbf{w}_k\|^2 + H^2}, \tag{21}$$

the constraint (16c) becomes $0 \le G_k[n] \le G_{k,\max}[n], \forall k, n$. Besides, the achievable rate $R_k[n]$ in (14) can be rewritten by

$$R_k[n] = \log_2\left(1 + \sum_{m=1}^{K} G_m[n]\right) - \hat{R}_k[n], \tag{22}$$

where

$$\hat{R}_k[n] \triangleq \log_2\left(1 + \sum_{j=1,j\neq k}^{K} G_j[n]\right). \tag{23}$$

Then, by introducing auxiliary variables $\{V_{\text{lb}}[n]\}$, (P1) can be recast to

$$(P1.1):$$

$$\max_{\substack{\{\mathbf{q}[n],\mathbf{v}[n],\mathbf{a}[n]\} \\ \{G_k[n],V_{\text{lb}}[n],\tau\}}} \quad \tau \tag{24a}$$

$$s.t. \quad \frac{1}{N}\sum_{n=1}^{N}\left(\log_2\left(1 + \sum_{m=1}^{K} G_m[n]\right) - \hat{R}_k[n]\right) \ge \tau, \forall k, \tag{24b}$$

$$0 \le G_k[n] \le G_{k,\max}[n], \forall k, n, \tag{24c}$$

$$\frac{1}{N}\sum_{n=1}^{N} c_1\|\mathbf{v}[n]\|^3 + \frac{c_2}{V_{\text{lb}}[n]} + \frac{c_2\|\mathbf{a}[n]\|^2}{g^2 V_{\text{lb}}[n]} \le P_{\text{lim}}, \tag{24d}$$

$$V_{\min} \le V_{\text{lb}}[n], \forall n, \tag{24e}$$

$$V_{\text{lb}}^2[n] \le \|\mathbf{v}[n]\|^2, \forall n, \tag{24f}$$

$$\|\mathbf{v}[n]\| \le V_{\max}, \forall n, \tag{24g}$$

$$(6), (7), (8), (10).$$

It can be shown that at the optimal point of (P1.1), the inequality constraint in (24f) hold with equality since otherwise

we can enlarge the feasible set corresponding to (24d) by increasing $V_{\text{lb}}[n]$. Thus, we conclude that (P1.1) is equivalent to (P1). Thanks to the new auxiliary variables $\{V_{\text{lb}}[n]\}$, constraints (24d) and (24e) now become convex, while (24b), (24c), and (24f) are still non-convex in general.

To address these issues, we employ the SCA methods. First, it can be checked that constraint (24b) is given by a difference of two concave functions. Therefore, the surrogate function $\hat{R}_k^{\text{ub}}[n]$ for $\hat{R}_k[n]$ is computed from the first order Taylor approximation as

$$\hat{R}_k^{\text{ub}}[n] \triangleq \hat{\Gamma}_k[n]\left(\sum_{j=1,j\neq k}^{K}\left(G_{j,l+1}[n]-G_{j,l}[n]\right)\right) + \log_2\left(1+\sum_{j=1,j\neq k}^{K} G_{j,l}[n]\right) \geq \hat{R}_k[n], \quad (25)$$

where $G_{k,l}[n]$ denotes the solution of $G_k[n]$ attained at the l-th iteration of the SCA process and $\hat{\Gamma}_k[n]$ is defined as

$$\hat{\Gamma}_k[n] \triangleq \frac{\log_2 e}{1+\sum_{j=1,j\neq k}^{K} G_{j,l}[n]}, \forall k,n. \quad (26)$$

Next, to identify convex surrogate functions of (24c) and (24f), we present the following lemmas.

Lemma 1: Denoting $\{\mathbf{q}_l[n]\}$ as the solution for $\{\mathbf{q}[n]\}$ calculated at the l-th iteration, the surrogate function of $G_{k,\max}[n]$ can be expressed as

$$G_{k,\max}^{\text{lb}}[n] \triangleq P_{\text{peak}}\gamma_0\Big(-\frac{\|\mathbf{q}_{l+1}[n]-\mathbf{w}_k\|^2}{H^4} + B_k[n]\left(\mathbf{q}_{l+1}[n]-\mathbf{w}_k\right)^T\left(\mathbf{q}_l[n]-\mathbf{w}_k\right)+C_k[n]\Big) \leq G_{k,\max}[n], \quad (27)$$

where the constants $B_k[n]$ and $C_k[n]$ are respectively given as

$$B_k[n] \triangleq 2\left(\frac{1}{H^4}-\frac{1}{\left(\|\mathbf{q}_l[n]-\mathbf{w}_k\|^2+H^2\right)^2}\right), \forall k,n, \quad (28)$$

$$C_k[n] \triangleq \frac{1}{\|\mathbf{q}_l[n]-\mathbf{w}_k\|^2+H^2}+\frac{2\|\mathbf{q}_l[n]-\mathbf{w}_k\|^2}{\left(\|\mathbf{q}_l[n]-\mathbf{w}_k\|^2+H^2\right)^2} - \frac{\|\mathbf{q}_l[n]-\mathbf{w}_k\|^2}{H^4}, \forall k,n. \quad (29)$$

Proof: Please refer to Appendix A. ■

Lemma 2: With the solution $\{\mathbf{v}_l[n]\}$ obtained at the l-th iteration, the surrogate function of $\|\mathbf{v}_{l+1}[n]\|^2$ can be obtained as

$$-\|\mathbf{v}_{l+1}[n]\|^2+2\mathbf{v}_l^T\left(2\mathbf{v}_{l+1}[n]-\mathbf{v}_l[n]\right) \leq \|\mathbf{v}_{l+1}[n]\|^2. \quad (30)$$

Proof: Please refer to Appendix B. ■

With the aid of lemmas 1 and 2, at the l-th iteration, non-convex constraints (24c) and (24f) can be approximated as

$$0 \leq G_k[n] \leq G_{k,\max}^{\text{lb}}[n], \forall k,n, \quad (31)$$

$$V_{\text{lb}}^2[n] \leq -\|\mathbf{v}_{l+1}[n]\|^2+2\mathbf{v}_l^T\left(2\mathbf{v}_{l+1}[n]-\mathbf{v}_l[n]\right), \forall n. \quad (32)$$

As a result, with given $\{\mathbf{q}_l[n],\ \mathbf{v}_l[n],\ G_{k,l}[n]\}$, we solve the following problem at the l-th iteration of the SCA procedure

$$(P1.2):$$

$$\max_{\substack{\{\mathbf{q}_{l+1}[n],\mathbf{v}_{l+1}[n],\mathbf{a}[n]\}\\ \{G_{k,l+1}[n],V_{\text{lb}}[n],\tau\}}} \tau \quad (33a)$$

$$s.t.\ \frac{1}{N}\sum_{n=1}^{N}\left(\log_2\left(1+\sum_{m=1}^{K}G_{m,l+1}[n]\right)-\hat{R}_k^{\text{ub}}[n]\right) \geq \tau, \forall k, \quad (33b)$$

$$(6),(7),(8),(10),(24d),(24e),(24g),(31),(32).$$

Since (P1.2) is a convex optimization problem, it can be optimally solved convex optimization solvers such as the CVX [19]. The iterative SCA procedure is summarized in Algorithm 1. The convergence of Algorithm 1 has been proved [17], and thus we can compute at least a locally optimal solution for (P1).

Algorithm 1 : Proposed algorithm for (P1)

1: Initialize $\{\mathbf{q}_0[n],\ \mathbf{v}_0[n],\ G_{k,0}[n]\}, \forall k,n$ which satisfying the constraints and let $l=0$.
2: **Repeat**
3: Solve problem (P1.2) for the given local point $\{\mathbf{q}_l[n],\ \mathbf{v}_l[n],\ G_{k,l}[n]\}$, and denote the optimal solutions as $\{\mathbf{q}_{l+1}[n],\ \mathbf{v}_{l+1}[n],\ G_{k,l+1}[n]\}, \forall k,n$.
4: Update $l \leftarrow l+1$.
5: **Until** Convergence.
6: Obtain $p_k[n]=\frac{G_{k,l+1}[n]}{h_k[n]}, \forall k,n$.

A. Initial Trajectory

For the proposed algorithm, we need to initialize the trajectory variables $\mathbf{q}_0[n]$. To this end, we consider a simple circular trajectory scheme as in [16] with a center $\mathbf{c}$ and a radius r_0. First, the center $\mathbf{c}=[x_0,y_0]^T$ is determined as the geometrical mean of the ground nodes, i.e., $\mathbf{c}=\frac{\sum_{k=1}^{K}\mathbf{w}_k}{K}$.

Next, the radius r_0 is chosen to fulfill the constraints (9), (10), and (16d), which are equivalently expressed as

$$\frac{V_{\min}T}{2\pi} \leq r_0 \leq \min\left(\frac{V_{\max}T}{2\pi}, \frac{a_{\max}}{\omega_0^2}\right), \quad (34)$$

$$c_1 r_0^3\omega_0^3+\frac{c_2}{r_0\omega_0}+\frac{c_2 r_0\omega_0^3}{g^2} \leq P_{\lim}, \quad (35)$$

with $\omega_0 \triangleq \frac{2\pi}{T}$. The closed-form solution of inequality (35) can be readily obtained by using quartic formula. Then, r_0 is given as the point which makes the maximum objective value of (P1) under satisfying (34) and (35). As a result, the initial circular trajectory $\mathbf{q}_0[n]$ is written by $\mathbf{q}_0[n]=[r_0\cos 2\pi\frac{n}{N}+x_0, r_0\sin 2\pi\frac{n}{N}+y_0]^T, \forall n$.

IV. Numerical Result

In this section, we provide numerical results to validate the efficiency of the proposed algorithm. For the simulations, we consider K = 6 ground nodes which are distributed as in Fig. 2. The UAV gets around over the nodes horizontally at a constant altitude H = 100 m. The reference SNR γ_0 is set to γ_0 = 80 dB and the peak transmission power P_{peak} at the

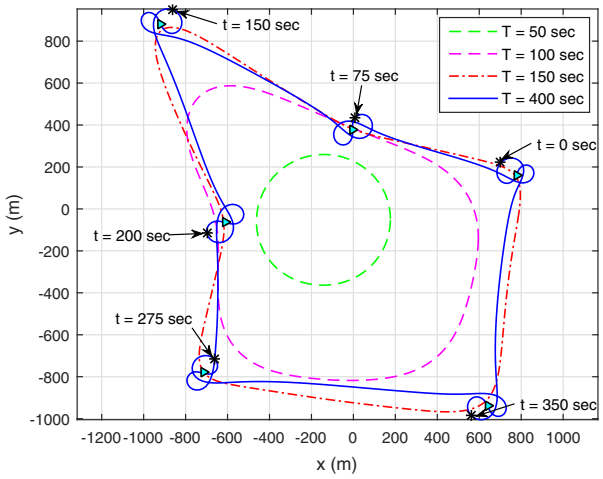

Fig. 2. Optimized UAV trajectories for different periods T given P_{lim} = 150 W. The ground node locations are marked with '▷'.

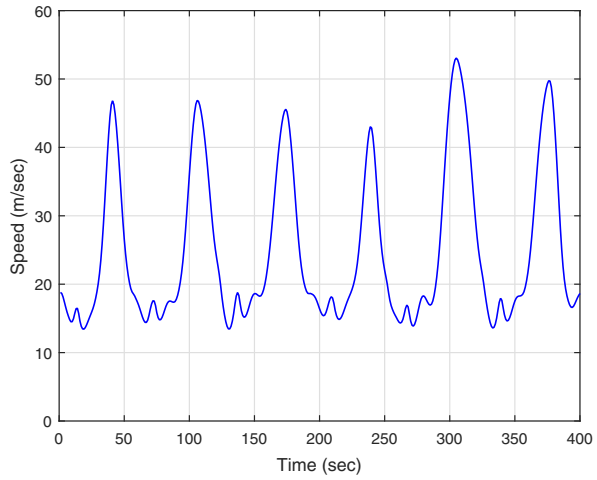

Fig. 3. The UAV speed versus time for T = 400 sec.

node is assumed to be $P_{\text{peak}} = 10$ dBm. The UAV's minimum velocity, maximum velocity, and maximum acceleration are set to $V_{\max} = 100$ m/sec, $V_{\min} = 3$ m/sec, and $a_{\max} = 5$ m/sec^2, respectively. For the UAV power consumption model in (14), the constants are fixed as $c_1 = 9.26 \times 10^{-4}$ and $c_2 = 2250$.

Fig. 2 illustrates the optimized UAV trajectories with various T for P_{lim} = 150 W. It is observed that when T is smaller than 150 sec, as T increases, the UAV tries to get closer to all the ground nodes in order to improve the channel conditions from the ground nodes. In contrast, if T is sufficiently large (T = 400 sec), the UAV is now able to visit all the nodes within a given time period. Thus, the UAV can hover over each node for a while by traveling smooth path around the nodes. This is an different observation presented in [16] where the practical UAV movement constraints (9), (10), and (16d) are not considered. This can be explained as follows: Since we consider the minimum velocity, the maximum acceleration,

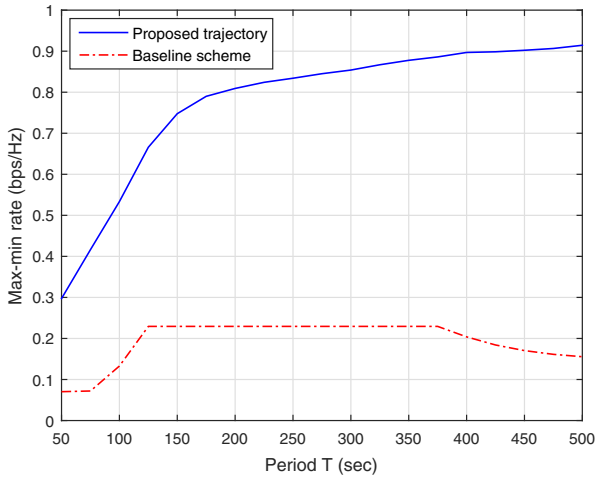

Fig. 4. Max-min rate versus period T given P_{lim} = 150 W.

and the propulsion power constraints, the UAV cannot stay at fixed positions as in [16]. Therefore, the UAV gets around over the node as close as possible to maintain good communication channel without exceeding propulsion power limit P_{lim}. We can also observe this result from Fig. 3, which the UAV flies between the nodes as fast as possible, while the UAV keeps low speed when it reached to the node.

Fig. 4 shows the average maximized minimum (max-min) rate obtained by the proposed algorithm and the baseline circular initialization scheme presented in section III-A as a function of T. First, it is observed that except for the T = 50 sec case which is strongly bounded by the acceleration constraint, the UAV fully exploits given propulsion power limit P_{lim} at the proposed trajectory. Also, it can be verified that the proposed trajectory optimization outperforms the baseline scheme regardless of the time period T. Moreover, we can see that the max-min rate with proposed trajectory monotonically increases as T grows, since the UAV can hover longer with a large T. In contrast, in the baseline scheme which is restricted in circular shape trajectory, the max-min rate first increase and then decreases after a certain time period. This can be explained that in order to satisfy the propulsion power constraint, the radius of the circular trajectory should increase as T gets large, which results in communication performance degradation. Therefore, we can conclude that the proposed trajectory becomes more powerful as the period T grows.

V. Conclusion

This paper has studied the UAV-aided wireless communication optimization under the propulsion energy consumption of the UAV. Specifically, to maximize the minimum average rate, the UAV trajectory and the ground nodes' uplink transmit power have been jointly optimized. The efficient iterative algorithm has been proposed by applying the SCA technique. Numerical results have demonstrated that the proposed algorithm provides substantial performance gains compared to the baseline scheme.

APPENDIX A
PROOF OF LEMMA 1

First, let us define a function $f_1(\mathbf{u})$ for $\mathbf{u} = [u_x \ u_y]^T$ as $f_1(\mathbf{u}) \triangleq \frac{1}{e\|\mathbf{u}\|^2+z}$ where $z > 0$ and $e > 0$ are constants. For any given $\mathbf{u}_l \in \mathbb{R}^{2\times 1}$, we also define the function $g_1(\mathbf{u}|\mathbf{u}_l)$ as

$$g_1(\mathbf{u}|\mathbf{u}_l) \triangleq -\frac{e\|\mathbf{u}\|^2}{z^2} + \overline{B}\mathbf{u}^T\mathbf{u}_l + \overline{C}, \tag{36}$$

where $\overline{B} \triangleq 2e\left(\frac{1}{z^2} - \frac{1}{(e\|\mathbf{u}_l\|^2+z)^2}\right)$ and $\overline{C} \triangleq \frac{1}{e\|\mathbf{u}_l\|^2+z} + \frac{2e\|\mathbf{u}_l\|^2}{(e\|\mathbf{u}_l\|^2+z)^2} - \frac{e\|\mathbf{u}_l\|^2}{z^2}$. Then, it can be easily shown that $f_1(\mathbf{u}_l) = g_1(\mathbf{u}_l|\mathbf{u}_l)$, i.e., $g_1(\mathbf{u}|\mathbf{u}_l)$ in (36) fulfils the condition in (17) of the surrogate function.

Also, the gradient of $f_1(\mathbf{u})$ and $g_1(\mathbf{u}|\mathbf{u}_l)$ with respect to $\mathbf{u}$ are respectively computed as

$$\nabla_{\mathbf{u}} f_1(\mathbf{u}) = -\frac{-2e\mathbf{u}}{(e\|\mathbf{u}\|^2+z)^2}, \tag{37}$$

$$\nabla_{\mathbf{u}} g_1(\mathbf{u}|\mathbf{u}_l) = -\frac{2e\mathbf{u}}{z^2} + \overline{B}\mathbf{u}_l. \tag{38}$$

The two gradients in (37) and (38) become identical at $\mathbf{u} = \mathbf{u}_l$, and thus $g_1(\mathbf{u}|\mathbf{u}_l)$ satisfies the second condition (18).

To prove the lower bound condition in (19), let us calculate the Hessian matrix of $h_1(\mathbf{u}|\mathbf{u}_l) \triangleq f_1(\mathbf{u}) - g_1(\mathbf{u}|\mathbf{u}_l)$ as

$$\nabla^2_{\mathbf{u}} h_1(\mathbf{u}|\mathbf{u}_l) = D\begin{bmatrix} E + 4ez^2u_x^2 & 4ez^2u_xu_y \\ 4ez^2u_xu_y & E + 4ez^2u_y^2 \end{bmatrix}, \tag{39}$$

where $D \triangleq \frac{2e}{z^2(e\|\mathbf{u}\|^2+z)^3} > 0$ and $E \triangleq e^3\|\mathbf{u}\|^6 + 3e^2z\|\mathbf{u}\|^4 + 2ez^2\|\mathbf{u}\|^2 \geq 0$. One can easily check that the Hessian in (39) is a positive semi-definite matrix, which implies that $h_1(\mathbf{u}|\mathbf{u}_l)$ is a convex function. Since $\nabla_{\mathbf{u}} h_1(\mathbf{u}|\mathbf{u}_l) = \mathbf{0}$ at $\mathbf{u} = \mathbf{u}_l$ from (37) and (38), the global minimum of $h_1(\mathbf{u}|\mathbf{u}_l)$ is achieved at $\mathbf{u} = \mathbf{u}_l$ with $h_1(\mathbf{u}_l|\mathbf{u}_l) = 0$. As a result, we can show that $h_1(\mathbf{u}|\mathbf{u}_l) \geq 0$ for any given $\mathbf{u}_l$, and thus the third condition in (19) for the surrogate function is hold. By substituting $\mathbf{u} = \mathbf{q}_{l+1}[n] - \mathbf{w}_k$, $\mathbf{u}_l = \mathbf{q}_l[n] - \mathbf{w}_k$, $z = H^2$, $e = 1$ and multiply $f_1(\mathbf{u})$ and $g_1(\mathbf{u}|\mathbf{u}_l)$ by $P_{\text{peak}}\gamma_0$, Lemma 1 is thus proved.

APPENDIX B
PROOF OF LEMMA 2

By denoting function $f_2(\mathbf{u})$ and $g_2(\mathbf{u}|\mathbf{u}_l)$ as

$$f_2(\mathbf{u}) \triangleq \|\mathbf{u}\|^2, \tag{40}$$

$$g_2(\mathbf{u}|\mathbf{u}_l) \triangleq -\|\mathbf{u}\|^2 + 2\mathbf{u}_l^T(2\mathbf{u} - \mathbf{u}_l), \tag{41}$$

we can easily verify that $f_2(\mathbf{u}_l) = g_2(\mathbf{u}_l|\mathbf{u}_l)$ and $\nabla_{\mathbf{u}} f_2(\mathbf{u}) = \nabla_{\mathbf{u}} g_2(\mathbf{u}|\mathbf{u}_l)$ at $\mathbf{u} = \mathbf{u}_l$.

In addition, similar to the proof of Lemma 1, it can be shown that a function $h_2(\mathbf{u}|\mathbf{u}_l) \triangleq f_2(\mathbf{u}) - g_2(\mathbf{u}|\mathbf{u}_l)$ is convex. Then, we have $\nabla_{\mathbf{u}} h_2(\mathbf{u}|\mathbf{u}_l) = \mathbf{0}$ at $\mathbf{u} = \mathbf{u}_l$, which indicates that the global minimum of $h_2(\mathbf{u}|\mathbf{u}_l)$ is zero and obtained at $\mathbf{u} = \mathbf{u}_l$. Thus, it follows $h_2(\mathbf{u}|\mathbf{u}_l) \geq 0$ for any given $\mathbf{u}_l$. Hence, we can obtain Lemma 2 by setting $\mathbf{u} = \mathbf{v}_{l+1}[n]$ and $\mathbf{u}_l = \mathbf{v}_l[n]$, This completes the proof.

REFERENCES

[1] Y. Zeng, R. Zhang, and T. J. Lim, "Wireless communications with unmanned aerial vehicles: opportunities and challenges," *IEEE Commun. Mag.*, vol. 54, pp. 36–42, May. 2016.

[2] W. Lee, I. Lee, J. S. Kwak, B.-C. Ihm, and S. Han, "Multi-BS MIMO cooperation: challenges and practical solutions in 4G systems," *IEEE Wireless Commun.*, vol. 19, pp. 89–96, Feb. 2012.

[3] Y. Zeng, R. Zhang, and T. J. Lim, "Throughput maximization for UAV-enabled mobile relaying systems," *IEEE Trans. Commun.*, vol. 64, pp. 4983–4996, Dec. 2016.

[4] Q. Wang, Z. Chen, W. Mei, and J. Fang, "Improving physical layer security using UAV-enabled mobile relaying," *IEEE Wireless Commun. Lett.*, vol. 6, pp. 310–313, Jun. 2017.

[5] D. H. Choi, S. H. Kim, and D. K. Sung, "Energy-efficient maneuvering and communication of a single UAV-based relay," *IEEE Trans. Aerosp. Electron. Syst.*, vol. 50, pp. 2320–2327, Jul. 2014.

[6] J. Zhang, Y. Zeng, and R. Zhang, "Spectrum and energy efficiency maximization in UAV-enabled mobile relaying," in *Proc. IEEE ICC*, pp. 1–6, May. 2017.

[7] C. Song, K.-J. Lee, and I. Lee, "Designs of MIMO amplify-and-forward wireless relaying networks: challenges and solutions," *IEEE Access*, vol. 5, pp. 9223–9234, May. 2017.

[8] H.-B. Kong, C. Song, H. Park, and I. Lee, "A new beamforming design for MIMO AF relaying systems with direct link," *IEEE Trans. Commun.*, vol. 62, pp. 2286–2295, Jul. 2014.

[9] A. Merwaday and I. Guvenc, "UAV assisted heterogeneous networks for public safety communications," in *Proc. IEEE WCNC*, pp. 329–334, May. 2015.

[10] J. Lyu, Y. Zeng, and R. Zhang, "Spectrum sharing and cyclical multiple access in UAV-aided cellular offloading," *arXiv preprint arXiv:1705.09024*, 2017.

[11] S. Jeong, O. Simeone, and J. Kang, "Mobile edge computing via a UAV-mounted cloudlet: optimization of bit allocation and path planning," *accepted in IEEE Trans. Veh. Technol.* [Online] Available: http://arxiv.org/abs/1609.05362.

[12] J. Xu, Y. Zeng, and R. Zhang, "UAV-enabled wireless power transfer: trajectory design and energy region characterization," *arXiv preprint arXiv:1706.07010*, 2017.

[13] A. Al-Hourani, S. Kandeepan, and S. Lardner, "Optimal LAP altitude for maximum coverage," *IEEE Wireless Commun. Lett.*, vol. 3, pp. 569–572, Jul. 2014.

[14] J. Lyu, Y. Zeng, R. Zhang, and T. J. Lim, "Placement optimization of UAV-mounted mobile base stations," *IEEE Commun. Lett.*, vol. 21, pp. 604–607, Mar. 2017.

[15] Y. Zeng and R. Zhang, "Energy-efficient UAV communication with trajectory optimization," *IEEE Trans. Wireless Commun.*, vol. 16, pp. 3747–3760, Jun. 2017.

[16] Q. Wu, Y. Zeng, and R. Zhang, "Joint trajectory and communication design for multi-UAV enabled wireless networks," *arXiv:1705.02723*, 2017.

[17] B. R. Marks and G. P. Wright, "A general inner approximation algorithm for nonconvex mathematical programs," *Operations Research*, vol. 26, pp. 681–683, Aug. 1978.

[18] Y. Sun, P. Babu, and D. P. Palomar, "Majorization-minimization algorithms in signal processing, communications, and machine learning," *IEEE Trans. Signal Process.*, vol. 65, pp. 794–816, Feb. 2017.

[19] M. Grant and S. Boyd, "CVX: Matlab software for disciplined convex programming, version 2.1." Available: http://cvxr.com/cvx, 2017.